# LIKELIHOOD CONTRIBUTION BASED MULTI-SCALE ARCHITECTURE FOR GENERATIVE FLOWS

Hari Prasanna Das, Pieter Abbeel & Costas J. Spanos

Department of Electrical Engineering and Computer Sciences University of California, Berkeley {hpdas, pabbeel, spanos}@eecs.berkeley.edu

## **ABSTRACT**

Deep generative modeling using flows has gained popularity owing to the tractable exact log-likelihood estimation with efficient training and synthesis process. However, flow models suffer from the challenge of having high dimensional latent space, same in dimension as the input space. An effective solution to the above challenge as proposed by Dinh et al. (2016) is a multi-scale architecture, which is based on iterative early factorization of a part of the total dimensions at regular intervals. Prior works on generative flows involving a multi-scale architecture perform the dimension factorization based on a static masking. We propose a novel multi-scale architecture that performs data dependent factorization to decide which dimensions should pass through more flow layers. To facilitate the same, we introduce a heuristic based on the contribution of each dimension to the total log-likelihood which encodes the importance of the dimensions. Our proposed heuristic is readily obtained as part of the flow training process, enabling versatile implementation of our likelihood contribution based multi-scale architecture for generic flow models. We present such an implementation for the original flow introduced in Dinh et al. (2016), and demonstrate improvements in log-likelihood score and sampling quality on standard image benchmarks. We also conduct ablation studies to compare proposed method with other options for dimension factorization.

#### 1 Introduction

Deep Generative Modeling aims to learn the embedded distributions and representations in input (especially unlabelled) data, requiring no/minimal human labelling effort. Learning without knowledge of labels (unsupervised learning) is of increasing importance because of the abundance of unlabelled data and the rich inherent patterns they posses. The representations learnt can then be utilized in a number of downstream tasks such as semi-supervised learning (Kingma et al., 2014; Odena, 2016), synthetic data augmentation and adversarial training (Cisse et al., 2017), text analysis and model based control etc. The repository of deep generative modeling majorly includes Likelihood based models such as autoregressive models (Oord et al., 2016b; Graves, 2013), latent variable models (Kingma & Welling, 2013), flow based models (Dinh et al., 2014; 2016; Kingma & Dhariwal, 2018) and implicit models such as generative adversarial networks (GANs) (Goodfellow et al., 2014). Autoregressive models (Salimans et al., 2017; Oord et al., 2016b;a; Chen et al., 2017) achieve exceptional log-likelihood score on many standard datasets, but suffer from slow sampling process, making them unacceptable to adopt in real world applications. Latent variable models such as variational autoencoders (Kingma & Welling, 2013) tend to better capture the global feature representation in data, but do not offer an exact density estimate. Implicit generative models such as GANs (Goodfellow et al., 2014) have recently become popular for their ability to synthesize realistic data (Karras et al., 2018; Engel et al., 2019). But, GANs do not offer a latent space suitable for downstream tasks, nor do they perform density estimation.

Flow based generative models (Dinh et al., 2016; Kingma & Dhariwal, 2018) perform exact density estimation with fast inference and sampling, due to their parallelizability. They also provide an information rich latent space suitable for many applications. However, the dimension of latent space for flow based generative models is same as the high-dimensional input space, by virtue of bijectivity nature of flows. This poses a bottleneck for flow models to scale with increasing input dimensions

due to computational complexity. An effective solution to the above challenge is a multi-scale architecture, introduced by Dinh et al. (2016), which performs iterative early gaussianization of a part of the total dimensions at regular intervals of flow layers. Many prior works including Kingma & Dhariwal (2018); Atanov et al. (2019); Durkan et al. (2019); Kumar et al. (2019) implement multi-scale architecture in their flow models, but use static masking methods for factorization of dimensions. We propose a multi-scale architecture which performs data dependent factorization to decide which dimensions should pass through more flow layers. For the decision making, we introduce a heuristic based on the amount of total log-likelihood contributed by each dimension, which in turn signifies their individual importance. We lay the ground rules for quantitative estimation and qualitative sampling to be satisfied by an ideal factorization method for a multi-scale architecture. Since in the proposed architecture, the heuristic is obtained as part of the flow training process, it can be universally applied to generic flow models. We present such an implementation for the flow model introduced in Dinh et al. (2016) and present quantitative and qualitative improvements. We also perform ablation studies to confirm the novelty of our method among possible options. Summing up, the contributions of our research are,

#### **Contributions:**

- A log-determinant based heuristic which entails the contribution by each dimensions towards the total log-likelihood in a multi-scale architecture.
- 2. A multi-scale architecture based on the above heuristic performing data-dependent splitting of dimensions, implemented for the flow model of Dinh et al. (2016)
- 3. Quantitative and qualitative analysis of above implementation and an ablation study

To the best of our knowledge, we are the first to propose a data-dependent splitting of dimensions in a multi-scale architecture.

#### 2 BACKGROUND

In this section, we illustrate the functioning of flow based generative models and the multiscale architecture as introduced by Dinh et al. (2016).

## 2.1 FLOW-BASED GENERATIVE MODELS

Let  $\mathbf{x}$  be a high-dimensional random vector with unknown true distribution  $\mathbf{x} \sim p(\mathbf{x})$ . The following formulation is directly applicable to continous data, and with some pre-processing steps such as dequantization (Uria et al., 2013; Salimans et al., 2017; Ho et al., 2019) to discrete data. Let  $\mathbf{z}$  be the latent variable with a known standard distribution  $p(\mathbf{z})$ , such as a standard multivariate gaussian. Using an i.i.d. dataset  $\mathcal{D}$ , the target is to model  $p_{\theta}(\mathbf{x})$  with parameters  $\theta$ . A flow,  $\mathbf{f}_{\theta}$  is defined to be an invertible transformation that maps observed data  $\mathbf{x}$  to the latent variable  $\mathbf{z}$ . A flow is invertible, so the inverse function  $\mathcal{T}$  maps  $\mathbf{z}$  to  $\mathbf{x}$ , i.e.

$$\mathbf{z} = \mathbf{f}_{\boldsymbol{\theta}}(\mathbf{x}) = \mathcal{T}^{-1}(\mathbf{x}) \text{ and } \mathbf{x} = \mathcal{T}(\mathbf{z}) = \mathbf{f}_{\boldsymbol{\theta}}^{-1}(\mathbf{z})$$
 (1)

The log-likelihood can be expressed as,

$$\log(p_{\theta}(\mathbf{x})) = \log(p(\mathbf{z})) + \log\left(\left|\det\left(\frac{\partial \mathbf{f}_{\theta}(\mathbf{x})}{\partial \mathbf{x}^{T}}\right)\right|\right)$$
(2)

where  $\frac{\partial \mathbf{f}_{\theta}(\mathbf{x})}{\partial \mathbf{x}^T}$  is the jacobian of  $\mathbf{f}_{\theta}$  at  $\mathbf{x}$ .

The invertibile nature of flow allows it to be capable of being composed of other flows of compatible dimensions. In practice, flows are constructed by composing a series of component flows. Let the flow  $\mathbf{f}_{\theta}$  be composed of K component flows, i.e.  $\mathbf{f}_{\theta} = \mathbf{f}_{\theta_K} \circ \mathbf{f}_{\theta_{K-1}} \circ \cdots \circ \mathbf{f}_{\theta_1}$  and the intermediate variables be denoted by  $\mathbf{y}_K, \mathbf{y}_{K-1}, \cdots, \mathbf{y}_0 = \mathbf{x}$ . Then the log-likelihood of the composed flow is,

$$\log(p_{\boldsymbol{\theta}}(\mathbf{x})) = \log(p(\mathbf{z})) + \log\left(\left|\det\left(\frac{\partial(\mathbf{f}_{\theta_K} \circ \mathbf{f}_{\theta_{K-1}} \circ \cdots \circ \mathbf{f}_{\theta_1}(\mathbf{x}))}{\partial \mathbf{x}^T}\right)\right|\right)$$
(3)

$$= \underbrace{\log(p(\mathbf{z}))}_{\text{Log-latent density}} + \sum_{i=1}^{K} \underbrace{\log|\det(\partial \mathbf{y}_i/\partial \mathbf{y}_{i-1}^T)|}_{\text{Log-det}}$$
(4)

which follows from the fact that  $\det(A \cdot B) = \det(A) \cdot \det(B)$ . In our work, we refer the first term in Equation 4 as  $\log$ -latent-density and the second term as  $\log$ -determinant ( $\log$ -det). The reverse path, from  $\mathbf{z}$  to  $\mathbf{x}$  can be written as a composition of inverse flows,  $\mathbf{x} = \mathbf{f}_{\theta}^{-1}(\mathbf{z}) = \mathbf{f}_{\theta_1}^{-1} \circ \mathbf{f}_{\theta_2}^{-1} \circ \cdots \circ \mathbf{f}_{\theta_K}^{-1}(\mathbf{z})$ . Confirming with the properties of a flow as mentioned above, different types of flows can be constructed (Kingma & Dhariwal, 2018; Dinh et al., 2016; 2014; Bell & Sejnowski, 1995). One flow of particular interest is affine flow, which we use in our work as it has tractable log-determinant and efficient inference and sampling. We refer interested readers to Dinh et al. (2016) for more details.

#### 2.2 Multi-scale Architecture

Multi-scale architecture is a design choice for latent space dimensionality reduction of flow models, in which part of the dimensions are factored out/early gaussianized at regular intervals, and the other part is exposed to more flow layers. The process is called dimension factorization. In the problem setting as introduced in Section 2.1, the factoring operation can be mathematically expressed as,

$$\mathbf{y}_0 = \mathbf{x} \tag{5}$$

$$\mathbf{z}_{l+1}, \mathbf{y}_{l+1} = \mathbf{f}_{\theta_{l+1}}(\mathbf{y}_l), \ l \in \{0, 1, \dots, K-2\}$$
 (6)

$$\mathbf{z}_K = \mathbf{f}_{\theta_K}(\mathbf{y}_{K-1}) \tag{7}$$

$$\mathbf{z} = (\mathbf{z}_1, \mathbf{z}_2, \cdots, \mathbf{z}_K) \tag{8}$$

The factoring of dimensions at early layers has the benefit of distributing the loss function throughout the network (Dinh et al., 2016) and optimizing the amount of computation and memory used by the model. We consider the multi-scale architecture for flow based generative models as introduced by Dinh et al. (2016) (and later used by state-of-the-art flow models such as Glow(Kingma & Dhariwal, 2018)) as the base of our research work.

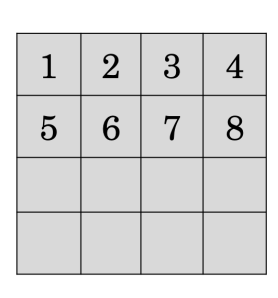
#### 3 LIKELIHOOD CONTRIBUTION BASED MULTISCALE ARCHITECTURE

In a multi-scale architecture, it is apparent that the variables getting exposed to more layers of flow will be more expressive in nature as compared to the ones which get factored at a finer scale (earlier layer). The method of splitting proposed by prior works such as (Dinh et al., 2016; Kingma & Dhariwal, 2018) are static in nature and do not distinguish between importance of different dimensions. In this section, we introduce a heuristic to estimate the contribution of each dimension towards the total log-likelihood, and introduce a method which can use the heuristic to decide the dimensions to be factored at an earlier layer, eventually achieving preferrential splitting in multiscale architecture. Our approach builds an efficient multiscale architecture which factors the dimensions at each flow layer in a way such that the local variance in the input space is well captured as the flow progresses and the log-likelihood is maximized. We also describe how our multi-scale architecture can be implemented over the flow model in RealNVP (Dinh et al., 2016).

Recall from Equation 4 that the log-likelihood is composed of two terms, the log-latent-density term and the log-det term. The log-latent-density term depends on the choice of latent distribution and is fixed given the sampled latent variable. Whereas, the log-det term depends on the modeling of the flow layers. So, once the latent variable is sampled, maximizing the log-det term results in maximized likelihood. The total log-det term is nothing but the sum of log-det terms contributed by each dimension. Let the dimension of the input space  $\mathbf{x}$  be  $s \times s \times c$ , where s is the image height/width and c is the number of channels for image inputs. For the following formulation, let us assume no dimensions were gaussianized early, so that we have access to log-det term for all dimensions at each flow layer. We apply a flow  $(\mathbf{f}_{\theta})$  with K component flows to  $\mathbf{x}$ ,  $\mathbf{z}$  pair, so that  $\mathbf{z} = \mathbf{f}_{\theta}(\mathbf{x}) = \mathbf{f}_{\theta_K} \circ \mathbf{f}_{\theta_{K-1}} \circ \cdots \circ \mathbf{f}_{\theta_1}(\mathbf{x})$ . The intermediate variables are denoted by  $\mathbf{y}_K, \mathbf{y}_{K-1}, \cdots, \mathbf{y}_0$  with  $\mathbf{y}_K = \mathbf{z}$  (since no early gaussianization was done) and  $\mathbf{y}_0 = \mathbf{x}$ . The log-det term at layer l,  $L_d^{(l)}$ , is given by,

$$[L_d^{(l)}]_{s \times s \times c} = \sum_{i=1}^{l} \log |\det(\partial \mathbf{y}_i / \partial \mathbf{y}_{i-1}^T)|$$
(9)

where,  $[L_d^{(l)}]_{s \times s \times c}$  denotes the log-det viewed as a  $s \times s \times c$  tensor corresponding to each of the variables, summed over the flow layers till l. Each of the terms in  $L_d^{(l)}$  can be considered as the



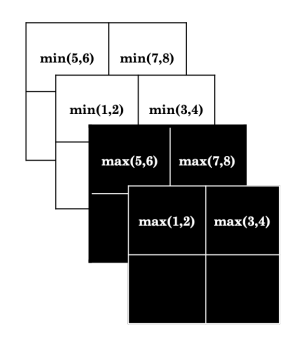


Figure 1: Likelihood contribution based squeezing operation for RealNVP: (On left) The tensor representing log-det of variables in a flow layer  $(s \times s \times c)$ . It is squeezed to  $\frac{s}{2} \times \frac{s}{2} \times 4c$  with local max and min pooling operation. (On right) The black (white) marked pixels represent dimensions having more (less) log-det locally.

contribution by the variable (dimension) towards the total log-det ( $\sim$  total log-likelihood). The entries having higher value correspond to the variables which contribute more towards the total log-likelihood, hence are more valuable for better flow formulation. So, we can use the *likelihood contribution* (in form of log-det term) by each dimension as a heuristic for deciding which variables should be gaussianized early in a multi-scale architecture. Ideally, at each flow layer, the variables with more log-det term should be exposed to more layer of flow and the ones having less log-det term should be factored out. In this manner, selectively more power can be provided to variables which capture meaningful representation (and are more valuable from log-det perspective) to be expressive by being exposed to multiple flow layers. This formulation leads to enhanced density estimation performance. Additionally, for many datasets such as images, the spatial nature should be taken into account while deciding dimensions for early gaussianization. Summarily, at every flow layer, an ideal factorization method should,

- 1. (Quantitative) For efficient density estimation: Early gaussianize the variables having less log-det and expose the ones having more log-det to more flow layers
- 2. (*Qualitative*) For qualitative reconstruction: Capture the local variance over the flow layers, i.e. the dimensions being exposed to more flow layers should contain representative pixel variables from throughout the whole image.

Keeping the above requirements in mind, variants of hybrid techniques for factorization could be implemented for different types of flow models which involve a multi-scale architecture, to improve their density estimation and qualitative performance. We refer to it as Likelihood Contribution based Multi-scale Architecture (LCMA). We describe an implementation of LCMA for affine flow as introduced in RealNVP (Dinh et al., 2016). Nevertheless, such an analogy can be extended for other flow models which involve a multiscale architecture, such as Glow (Kingma & Dhariwal, 2018).

For RealNVP, we propose a factorization method which converts the  $s \times s \times c$  shaped tensor  $[L_d^{(l)}]$ into a  $\frac{s}{2} \times \frac{s}{2} \times 4c$  shaped tensor using local max-pooling and min-pooling (= -max-pooling(-input)) operations, as illustrated in Figure 1 at each flow layer. Among the 4c channels, one half contains the dimensions having more log-det term compared with its neighbourhood pixel (Black marked in Fig. 1), while the other half contains the dimensions having less log-det (White marked in Fig. 1). Note that by grouping the dimensions having more/less log-det locally, we preserve the local spatial variation of the image in both parts of the factorization, which helps in qualitative reconstruction. Finally, the tensor is split along the channel dimension, followed by forwarding the dimensions contributing more to likelihood into more flow layers and early gaussianizing the ones contributing less. The proposed method factorizes the dimensions at each flow layer based on the log-det term available at that layer. So, we pre-train a network with no multiscale architecture (no dimensionality reduction) to obtain the log-det term at every flow layer. Then the dimensions to be factored at each flow layer is decided based on the log-det term at that layer, using proposed method. Only the dimensions that are chosen to be passed on to next layer of flow will be considered for applying the above method again at the next layer, e.g. for RealNVP, after a  $\frac{s}{2} \times \frac{s}{2} \times 2c$  tensor is factored from original  $s \times s \times c$  tensor, in the next layer, a  $\frac{s}{4} \times \frac{s}{4} \times 4c$  tensor will be factored specifically from the

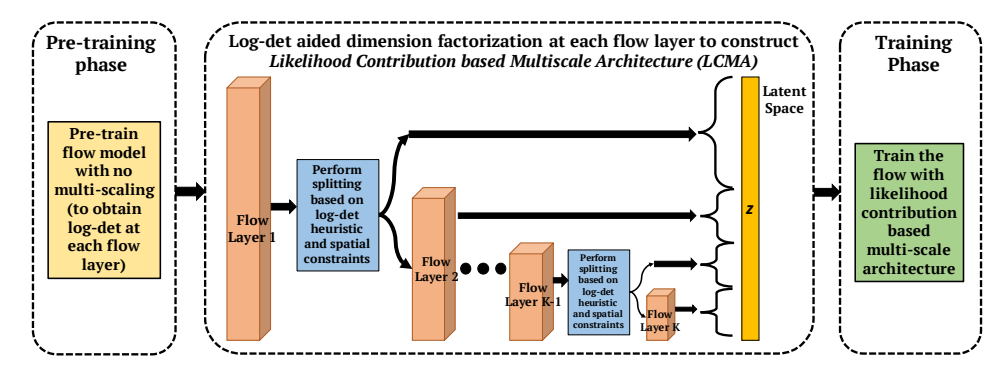


Figure 2: Illustration of proposed likelihood contribution based multi-scale architecture and associated training steps. Note that the dimension factorization step (middle box) is performed before the training phase, allowing use of non-invertible operations along with log-det heuristic.

 $\frac{s}{2} \times \frac{s}{2} \times 2c$  tensor which was exposed to more flow layers, inline with the recursive equation 6. This process is continued for all the layers till the latent space (gaussian). The decision of dimensions to be factored at each layer is done before training a network with multiscale architecture, and remains fixed once decided. Since the factorization of dimension does not occur online (during the training time), and before the actual training starts, the decision of dimensions which get factored at each flow layer is fixed, the change of variables formula can be applied. This allows the use of non-invertible operations (e.g. max and min pooling for RealNVP) for efficient factorization process along with log-det heuristic. The steps of proposed method are illustrated in Figure 2.

#### 4 RELATED WORK

Multi-scale architecture and variants have been successful in a number of prior works in deep generative modeling. For invertible neural networks, Finzi et al. (2019) use a keepChannel for selective feed forward of channels analogous to multi-scaling. In the spectrum of generative flow models, multi-scale architecture has been utilized to achieve the dimensionality reduction and enhanced training because of the distribution of loss function in the network (Dinh et al., 2016; Kingma & Dhariwal, 2018). A variant of multiscale architecture has been utilized to capture local variations in auto-regressive models (Reed et al., 2017). Among GAN(Goodfellow et al., 2014) models, Denton et al. (2015) use a multiscale variant to generate images in a coarse-to-fine manner. For multi-scale architectures in generative flow models, our proposed method performs factorization of dimensions based on their likelihood contribution, which in another sense translates to determining which dimensions are important from density estimation and qualitative reconstruction point of view. Keeping this in mind, we discuss prior works on generative flow models which involve multi-scaling and/or incorporate permutation among dimensions to capture their interactions.

A number of generative flow models implement a multi-scale architecture, such as Dinh et al. (2016); Kingma & Dhariwal (2018); Atanov et al. (2019); Izmailov et al. (2019); Durkan et al. (2019); Kumar et al. (2019) etc. Kingma & Dhariwal (2018) introduce an  $1 \times 1$  convolution layer in between the actnorm and affine coupling layer in their flow architecture. The  $1 \times 1$  convolution is a generalization of permutation operation which ensures that each dimension can affect every other dimension. This can be interpreted as redistributing the contribution of dimensions to total likelihood among the whole space of dimensions. So Kingma & Dhariwal (2018) treat the dimensions as equiprobable for factorization in their implementation of multi-scale architecture, and split the tensor at each flow layer evenly along the channel dimension. We, on the other hand, take the next step and focus on the individuality of dimensions and their importance from the amount they contribute towards the total log-likelihood. The log-det score is available readily as part of computations in a flow, so we essentially have a heuristic for free. Since our method focuses individually on the dimensions using a heuristic which is always available in flow model training, it can prove to be have more versatility in being compatible with generic multi-scale architectures, unlike Kingma & Dhariwal (2018) which relies on  $1 \times 1$  convolutions. Hoogeboom et al. (2019) extend the concept of  $1 \times 1$  convolutions to invertible  $d \times d$  convolutions, but do not discuss about multi-scaling. Dinh et al. (2016) also include

a type of permutation which is equivalent to reversing the ordering of the channels, but is more restrictive and fixed. Izmailov et al. (2019); Durkan et al. (2019); Kumar et al. (2019); Atanov et al. (2019) use multi-scale architecture in their flow models, coherent with Dinh et al. (2016); Kingma & Dhariwal (2018), but perform the factorization of dimensions without any consideration of the individual contribution of the dimension towards the total log-likelihood. For qualitative sampling along with efficient density estimation, we also propose that factorization methods should preserve spatiality of the image in the two splits, motivated by the spatial nature of splitting methods in Kingma & Dhariwal (2018) (channel-wise splitting) and Dinh et al. (2016) (checkerboard and channel-wise splitting).

#### 5 EXPERIMENTS

In Section 3, we established that our proposed likelihood contribution based factorization of dimensions can be implemented for flow models involving a multi-scale architecture, in order to improve their density estimation and qualitative performance. In this section we present the results of proposed Likelihood Contribution based Multiscale Architecture (LCMA) adopted for the flow model of RealNVP (Dinh et al., 2016). For direct comparison with results in Dinh et al. (2016), all the experimental settings such as data pre-processing, optimizer parameters as well as flow architectural details (coupling layers, residual blocks) are kept the same, except that the factorization of dimensions at each flow layer is performed according to the method described in Section 3. For ease of access, we also have summarized the details of experimental settings in Appendix A.

We perform experiments on four benchmarked image datasets: CIFAR-10 (Krizhevsky, 2009), Imagenet (Russakovsky et al., 2014) (downsampled to  $32 \times 32$  and  $64 \times 64$ ), and CelebFaces Attributes (CelebA) (Liu et al., 2015). The scaling in LCMA is performed once for CIFAR-10, thrice for Imagenet  $32 \times 32$  and 4 times for Imagenet  $64 \times 64$  and CelebA. For each dataset, we first pre-train the network without any multi-scaling (no dimensionality reduction in any flow layer) to obtain the log-det at each flow layer. Then the decision of dimensions to be factored at each layer is done as per the proposed method in Section 3. The final training is performed with the LCMA.

We compare LCMA with conventional multi-scale architecture and report the quantitative and qualitative results. We also perform an ablation study, whose results are summarized in Section 5.3.

#### 5.1 QUANTITATIVE COMPARISON

The bits/dim scores of RealNVP with conventional multi-scale architecture (as introduced in Dinh et al. (2016)) and RealNVP with LCMA are given in Table 1. It can be observed that the density estimation results using LCMA is in all cases better in comparison to the baseline. We observed that the improvement for CelebA is relatively high as compared to natural image datasets like CIFAR-10 or Imagenet. This observation was expected as facial features often contain high redundancy and the flow model learns to put more importance (reflected in terms of high log-det) on selected dimensions that define the facial features. Our proposed LCMA exposes such dimensions to more flow layers, making them more expressive and hence the significant improvement in code length (bits/dim) is observed. The improvement in code length is less for natural image datasets because of the high variance among features defining them, which has been the challenge with image compression algorithms. Note that the improvement in density estimation is always relative to the original flow architecture (RealNVP in our case) over which we use our proposed LCMA, as we do not alter any architecture other than the dimension factorization method.

Table 1: Improvements in density estimation (in bits/dim) using proposed method for RealNVP

| Model   | CelebA | CIFAR-10 | ImageNet 32x32 | ImageNet<br>64x64 |
|---|--------|----------|----------------|-------------------|
| RealNVP (Dinh et al., 2016)   | 3.02   | 3.49     | 4.28           | 3.98              |
| RealNVP flow model with Likelihood<br>Contribution based Multiscale Architecture (ours) | 2.71   | 3.43     | 4.21           | 3.92              |

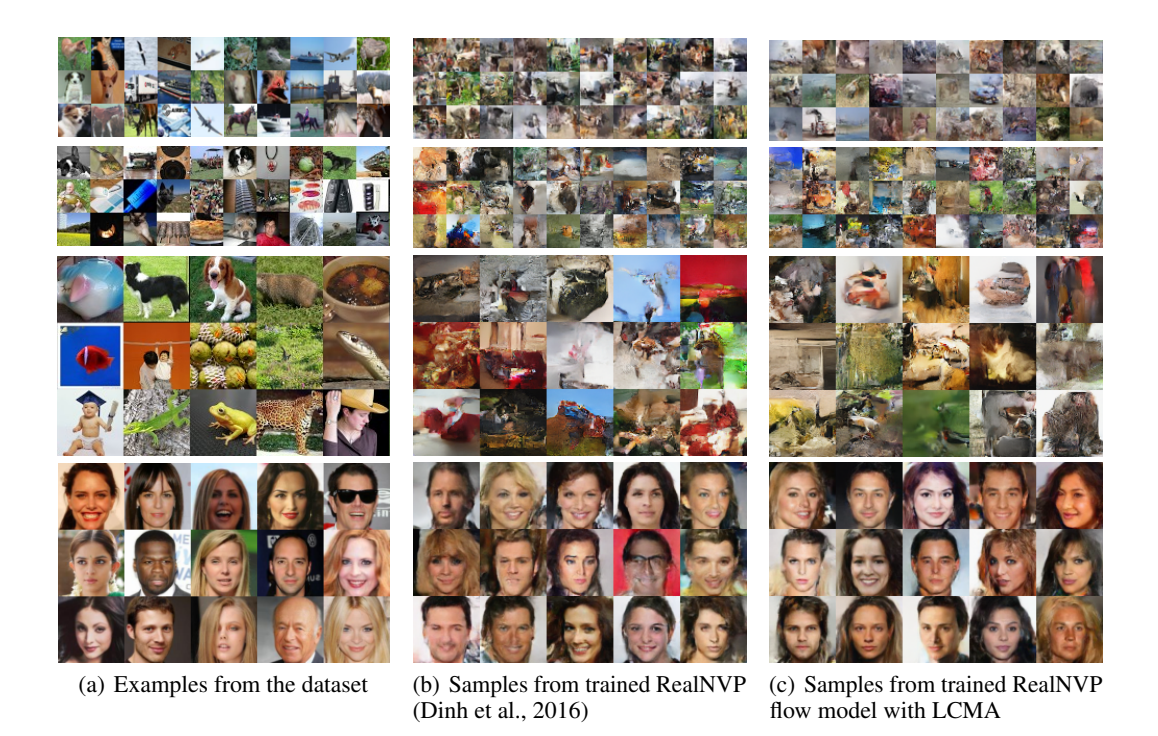


Figure 3: Samples from RealNVP (Dinh et al., 2016) and RealNVP flow model with proposed likelihood contribution based multiscale architecture (LCMA) trained on different datasets. The datasets shown in this figure are in order: CIFAR-10, Imagenet( $32 \times 32$ ), Imagenet ( $64 \times 64$ ) and CelebA (without low-temperature sampling). Additional samples are included in Appendix C.

#### 5.2 QUALITATIVE COMPARISON

An ideal dimension factorization method should capture the local variance over series of flow layers, which helps in qualitative sampling. For LCMA implementation with RealNVP, we introduced local max and min pooling operations on log-det heuristic to decide which dimensions to be gaussianized early (Section 3). Figure 3(a) shows samples from original datasets, Figure 3(b) shows the samples from trained RealNVP flow model with conventional multi-scale architecture (Dinh et al., 2016) and Figure 3(c) shows the samples from RealNVP flow with LCMA trained on various datasets. The finer facial details such as hair styles, eye-lining and facial folds in Celeba samples generated from RealNVP with LCMA were perceptually better than the baseline. The global feature representation observed is similar to that in (Dinh et al., 2016), as the flow architecture was kept the same. The background for natural images such as Imagenet  $32 \times 32$  and  $64 \times 64$  was constructed at par with the original flow model. As has been observed in different flow models such as Dinh et al. (2016); Kingma & Dhariwal (2018), the latent space holds knowledge about the feature representation in the data. The construction of latent space is affected by the dimension factorization method in a



Figure 4: Smooth linear interpolations in latent space between two images from CelebA dataset (without low-temperature sampling). The intermediate samples perceptibly resemble synthetic faces.

Table 2: Ablation study results for multi-scale architectures with various factorization methods

| Evaluations                           | Fixed Random<br>Permutation | Multiscale architecture<br>with early gaussianization of<br>high log-det dimensions | RealNVP<br>(Dinh et al., 2016) | Multiscale architecture<br>with early gaussianization of<br>low log-det dimensions |  |
|---------------------------------------|-----------------------------|---|--------------------------------|--|--|
| Quantitative<br>Evaluation (Bits/dim) | 3.05                        | 3.10  | 3.02                           | 2.71   |  |
| Qualitative<br>Evaluation             |                             |   |                                |  |  |

multi-scale architecture, since the variables which get gaussianized early directly constitute part of the latent space. To ensure efficient construction of latent space with our proposed LCMA, we observed interpolations among the image data. We took a pair of images from CelebA dataset, obtained their representation in latent space, performed a linear interpolation between the latent codes and generated the interpolation samples, as shown in Figure 4. The interpolations observed were smooth, with intermediate samples perceptibly resembling synthetic faces, signifying the efficient construction of latent space. More interpolations are included in Appendix B.

#### 5.3 ABLATION STUDY

We performed ablation studies to compare LCMA with other methods for dimension factorization in a multi-scale architecture. We consider 4 variants for our study, namely fixed random permutation, multiscale architecture with early gaussianization of high log-det dimensions, factorization method with checker-board and channel splitting as introduced in Dinh et al. (2016) and multiscale architecture with early gaussianization of low log-det dimensions, which is our proposed LCMA. In fixed random permutation, we randomly partition a  $s \times s \times c$  tensor into two halves, with no regard to the spatiality or log-det score. In multiscale architecture with early gaussianization of high log-det dimensions, we do the reverse of the ordering in LCMA, and gaussianize the high log-det variables early. The bits/dim score and generated samples for each of the method are given in Table 2. As expected from an information theoretic perspective, gaussianizing high log-det variables early provides the worst density estimation, as the model could not capture the high amount of important information inherent in the variables. Comparing the same method with fixed random permutation, the latter has better score as the probability of a high log-det variable being gaussianized early reduces to half, and the probability gets further reduced with RealNVP due to channel-wise and checkerboard splitting. LCMA has the best score among all methods, as the variables carrying more information are exposed to more flow layers. Fixed random permutation has the worst quality of sampled images, as the spatiality is lost during factorization. The sample quality improves in multiscale architecture with early gaussianization of high log-det dimensions and RealNVP. The sampled images are perceptually best for LCMA among all the methods, as in this case, both spatiality and log-det score is taken into account. Summarizing, LCMA outperforms multi-scale architectures based on other factorization methods, as it improves density estimation and generates qualitative samples for generative flows.

#### 6 CONCLUSIONS AND FUTURE WORK

We proposed a novel multi-scale architecture for generative flows which employs a data-dependent splitting based the contribution of dimensions to the total log-likelihood. Implementations of the proposed method for the flow introduced in Dinh et al. (2016) was presented. Empirical studies conducted on benchmark image datasets validate the strength of our proposed method, which improves log-likelihood scores and is able to generate qualitative samples. Ablation study results confirm the power of LCMA over other options for dimension factorization. A line of future work can be to design/learn a masking scheme for factorization on the go during training (possibly a parallel training process), while preserving flow properties to further reduce the computation.

## REFERENCES

- Andrei Atanov, Alexandra Volokhova, Arsenii Ashukha, Ivan Sosnovik, and Dmitry Vetrov. Semiconditional normalizing flows for semi-supervised learning. *arXiv preprint arXiv:1905.00505*, 2019.
- A. J. Bell and T. J. Sejnowski. An information-maximization approach to blind separation and blind deconvolution. *Neural Computation*, 7(6):1129–1159, Nov 1995. ISSN 0899-7667. doi: 10.1162/neco.1995.7.6.1129.
- Xi Chen, Nikhil Mishra, Mostafa Rohaninejad, and Pieter Abbeel. Pixelsnail: An improved autoregressive generative model. *arXiv preprint arXiv:1712.09763*, 2017.
- Moustapha Cisse, Piotr Bojanowski, Edouard Grave, Yann Dauphin, and Nicolas Usunier. Parseval networks: Improving robustness to adversarial examples. In *Proceedings of the 34th International Conference on Machine Learning-Volume 70*, pp. 854–863. JMLR. org, 2017.
- Emily L Denton, Soumith Chintala, Rob Fergus, et al. Deep generative image models using a laplacian pyramid of adversarial networks. In *Advances in neural information processing systems*, pp. 1486–1494, 2015.
- Laurent Dinh, David Krueger, and Yoshua Bengio. Nice: Non-linear independent components estimation. *arXiv preprint arXiv:1410.8516*, 2014.
- Laurent Dinh, Jascha Sohl-Dickstein, and Samy Bengio. Density estimation using real NVP. *CoRR*, abs/1605.08803, 2016. URL http://arxiv.org/abs/1605.08803.
- Conor Durkan, Artur Bekasov, Iain Murray, and George Papamakarios. Cubic-spline flows. *arXiv* preprint arXiv:1906.02145, 2019.
- Jesse Engel, Kumar Krishna Agrawal, Shuo Chen, Ishaan Gulrajani, Chris Donahue, and Adam Roberts. Gansynth: Adversarial neural audio synthesis. *arXiv preprint arXiv:1902.08710*, 2019.
- Marc Finzi, Pavel Izmailov, Wesley Maddox, Polina Kirichenko, and Andrew Gordon Wilson. Invertible convolutional networks. In *Workshop on Invertible Neural Nets and Normalizing Flows, International Conference on Machine Learning*, 2019.
- Ian Goodfellow, Jean Pouget-Abadie, Mehdi Mirza, Bing Xu, David Warde-Farley, Sherjil Ozair, Aaron Courville, and Yoshua Bengio. Generative adversarial nets. In Advances in neural information processing systems, pp. 2672–2680, 2014.
- Alex Graves. Generating sequences with recurrent neural networks. arXiv preprint arXiv:1308.0850, 2013.
- Jonathan Ho, Xi Chen, Aravind Srinivas, Yan Duan, and Pieter Abbeel. Flow++: Improving flow-based generative models with variational dequantization and architecture design. arXiv preprint arXiv:1902.00275, 2019.
- Emiel Hoogeboom, Rianne van den Berg, and Max Welling. Emerging convolutions for generative normalizing flows. *arXiv preprint arXiv:1901.11137*, 2019.
- Pavel Izmailov, Polina Kirichenko, Marc Finzi, and Andrew Gordon Wilson. Semi-supervised learning with normalizing flows. In *Workshop on Invertible Neural Nets and Normalizing Flows, International Conference on Machine Learning*, 2019.
- Tero Karras, Samuli Laine, and Timo Aila. A style-based generator architecture for generative adversarial networks. *arXiv preprint arXiv:1812.04948*, 2018.
- Diederik P Kingma and Jimmy Ba. Adam: A method for stochastic optimization. *arXiv* preprint arXiv:1412.6980, 2014.
- Diederik P Kingma and Max Welling. Auto-encoding variational bayes. *arXiv preprint* arXiv:1312.6114, 2013.

- Durk P Kingma and Prafulla Dhariwal. Glow: Generative flow with invertible 1x1 convolutions. In *Advances in Neural Information Processing Systems*, pp. 10215–10224, 2018.
- Durk P Kingma, Shakir Mohamed, Danilo Jimenez Rezende, and Max Welling. Semi-supervised learning with deep generative models. In *Advances in neural information processing systems*, pp. 3581–3589, 2014.
- Alex Krizhevsky. Learning multiple layers of features from tiny images. Technical report, Citeseer, 2009.
- Manoj Kumar, Mohammad Babaeizadeh, Dumitru Erhan, Chelsea Finn, Sergey Levine, Laurent Dinh, and Durk Kingma. Videoflow: A flow-based generative model for video. *arXiv preprint arXiv:1903.01434*, 2019.
- Ziwei Liu, Ping Luo, Xiaogang Wang, and Xiaoou Tang. Deep learning face attributes in the wild. In *Proceedings of the IEEE international conference on computer vision*, pp. 3730–3738, 2015.
- Augustus Odena. Semi-supervised learning with generative adversarial networks. *arXiv preprint arXiv:1606.01583*, 2016.
- Aaron Van den Oord, Nal Kalchbrenner, Lasse Espeholt, Oriol Vinyals, Alex Graves, et al. Conditional image generation with pixelcnn decoders. In Advances in neural information processing systems, pp. 4790–4798, 2016a.
- Aaron van den Oord, Nal Kalchbrenner, and Koray Kavukcuoglu. Pixel recurrent neural networks. *arXiv preprint arXiv:1601.06759*, 2016b.
- Scott Reed, Aäron van den Oord, Nal Kalchbrenner, Sergio Gómez Colmenarejo, Ziyu Wang, Yutian Chen, Dan Belov, and Nando de Freitas. Parallel multiscale autoregressive density estimation. In *Proceedings of the 34th International Conference on Machine Learning-Volume 70*, pp. 2912–2921. JMLR. org, 2017.
- Olga Russakovsky, Jia Deng, Hao Su, Jonathan Krause, Sanjeev Satheesh, Sean Ma, Zhiheng Huang, Andrej Karpathy, Aditya Khosla, Michael S. Bernstein, Alexander C. Berg, and Fei-Fei Li. Imagenet large scale visual recognition challenge. *CoRR*, abs/1409.0575, 2014. URL http://arxiv.org/abs/1409.0575.
- Tim Salimans, Andrej Karpathy, Xi Chen, and Diederik P. Kingma. Pixelcnn++: Improving the pixelcnn with discretized logistic mixture likelihood and other modifications. *CoRR*, abs/1701.05517, 2017. URL http://arxiv.org/abs/1701.05517.
- Benigno Uria, Iain Murray, and Hugo Larochelle. Rnade: The real-valued neural autoregressive density-estimator. In *Advances in Neural Information Processing Systems*, pp. 2175–2183, 2013.

#### A EXPERIMENTAL SETTINGS

For direct comparison with Dinh et al. (2016), data pre-processing, optimizer parameters as well as flow architectural details (coupling layers, residual blocks) are kept the same, except that the factorization of dimensions at each flow layer is performed according to the method described in Section 3. In this section, for the ease of access, we summarize the experimental settings.

**Datasets:** We perform experiments on four benchmarked image datasets: CIFAR-10 (Krizhevsky, 2009), Imagenet (Russakovsky et al., 2014) (downsampled to  $32 \times 32$  and  $64 \times 64$ ), and CelebFaces Attributes (CelebA) (Liu et al., 2015).

**Pre-processing:** For CelebA, we take a central crop of  $148 \times 148$  then resize it to  $64 \times 64$ . For dequantization of images (whose values lies in  $[0,256]^D$ ), the data is transformed to  $\operatorname{logit}(\alpha+(1-\alpha)\odot\frac{x}{256})$ , where  $\alpha=0.05$ . The sample allocation for training and validation were done as per the official allocation for the datasets.

Flow model architecture: We use affine coupling layers as introduced (Dinh et al., 2016). A layer of flow is defined as 3 coupling layers with checkerboard splits at  $s \times s$  resolution, 3 coupling layers with channel splits at  $s/2 \times s/2$  resolution, where s is the resolution at the input of that layer. For datasets having resolution 32, we use 3 such layers and for those having resolution 64, we use 4 layers. The cascade connection of the layers is followed by 4 coupling layers with checkerboard splits at the final resolution, marking the end of flow composition. For CIFAR-10, each coupling layer uses 8 residual blocks. Other datasets having images of size  $32 \times 32$  use 4 residual blocks whereas  $64 \times 64$  ones use 2 residual blocks. More details on architectures will be given in a source code release.

**Optimization parameters**: We optimize with ADAM optimizer (Kingma & Ba, 2014) with default hyperparameters and use an  $L_2$  regularization on the weight scale parameters with coefficient  $5 \cdot 10^{-5}$ . A batch size of 64 was used. The computations were performed in NVIDIA Tesla V100 GPUs.

**Multiscale Architecture:** Scaling is done once for CIFAR-10, thrice for Imagenet  $32 \times 32$  and 4 times for Imagenet  $64 \times 64$  and CelebA.

#### B INTERPOLATIONS AMONG TWO IMAGES FROM CELEBA DATASET

Figure 5 presents more interpolation examples obtained using our model between two images from CelebA dataset.



Figure 5: Linear interpolations between two CelebA images (without low-temperature sampling)

# C ADDITIONAL SAMPLES

In this section, we present more samples from models with likelihood contribution based multiscale architecture trained on different datasets.



Figure 6: Samples from model trained on CIFAR-10 dataset



Figure 7: Samples from model trained on Imagenet  $32 \times 32$  dataset



Figure 8: Samples from model trained on Imagenet  $64 \times 64$  dataset



Figure 9: Samples from model trained on CelebA dataset without low-temperature sampling